

RSC Advances



This is an *Accepted Manuscript*, which has been through the Royal Society of Chemistry peer review process and has been accepted for publication.

Accepted Manuscripts are published online shortly after acceptance, before technical editing, formatting and proof reading. Using this free service, authors can make their results available to the community, in citable form, before we publish the edited article. This *Accepted Manuscript* will be replaced by the edited, formatted and paginated article as soon as this is available.

You can find more information about *Accepted Manuscripts* in the [Information for Authors](#).

Please note that technical editing may introduce minor changes to the text and/or graphics, which may alter content. The journal's standard [Terms & Conditions](#) and the [Ethical guidelines](#) still apply. In no event shall the Royal Society of Chemistry be held responsible for any errors or omissions in this *Accepted Manuscript* or any consequences arising from the use of any information it contains.

1 **Enhancing the charge separation and migration efficiency of**
2 **Bi₂WO₆ by hybridizing P3HT conducting polymer**

3 Tingting Zheng, Jiayue Xu*, Zhijie Zhang*, Haibo Zeng

4 School of Materials Science and Engineering, Shanghai Institute of Technology, 100

5 Haiquan Road, Shanghai, 201418, P.R. China

6 *Corresponding author. Tel.: +86-21-6087-3581; Fax: +86-21-6087-3439

7 *Email address:* xujiayue@sit.edu.cn (J. Xu); zjzhang@sit.edu.cn (Z. Zhang)

8
9 **Abstract:** In order to improve the charge separation and migration efficiency, a
10 conducting polymer, poly(3-hexylthiophene) (P3HT), was introduced into Bi₂WO₆
11 photocatalyst. The hall mobility of P3HT/Bi₂WO₆ composite and bare Bi₂WO₆ were
12 4.7197x10² cm²/Vs and 3.0159x10² cm²/Vs, respectively, indicating the high charge
13 transfer ability of the P3HT/Bi₂WO₆ composite. The photo-degradation of a model
14 pollutant, rhodamine B (RhB) under simulated solar light irradiation, demonstrated
15 that the P3HT/Bi₂WO₆ composite showed much enhanced photocatalytic activity than
16 bare Bi₂WO₆. The excellent photocatalytic performance of the P3HT/Bi₂WO₆
17 composite could be ascribed to the internal electric field formed between n-type
18 Bi₂WO₆ and p-type P3HT, which facilitates the separation of photo-generated
19 electron-hole pairs, as well as the high charge carrier mobility of P3HT, which can
20 transport the photo-generated holes to the surface of the semiconductor quickly to
21 participate in the oxidation of pollutants.

22 **Keywords:** Photocatalysis; Conducting polymer; Composites; Bi₂WO₆; P3HT

23

1

2 **1. Introduction**

3 With the increasing global environmental problems, the potential application of
4 photocatalysis in environmental purification has aroused widespread concern in the
5 past few decades [1, 2]. In principle, heterogeneous photocatalysis involves the
6 generation, separation and migration of photo-induced charge carriers, which undergo
7 redox reactions with the adsorbed substrates on the surface of the semiconductor [3,
8 4]. Desired photocatalysts are expected to promote the charge transfer process while
9 suppressing the recombination process. Unfortunately, due to the fast recombination
10 rate of photo-induced electron-hole pairs, the photocatalytic systems developed thus
11 far have been restricted by its low efficiency [5, 6]. Therefore, in order to expand the
12 application of photocatalysis, it is important to facilitate the charge separation and
13 migration rates. To date, great efforts have been made to increase the charge
14 separation efficiency, such as the loading of noble metals on the surface of the
15 photocatalyst as cocatalysts [7, 8], or forming a composite photocatalyst between two
16 kinds of semiconductors [9-14]. Another effective way to promote the charge
17 separation rate is hybridizing a conjugated polymer with the semiconductor
18 photocatalyst [15-17].

19 Conjugated polymers such as polythiophenes, polypyrroles, polyanilines,
20 poly(p-phenylenevinylene), and their derivatives are extensively employed in
21 photovoltaic devices as antenna layers for photovoltaic conversion of solar energy
22 [18-20]. In recent years, conjugated polymers have also been widely applied in
23 photocatalysis area to improve the photocatalytic properties of TiO₂. For example, Lin

1 et al. synthesized polyaniline (PANI)/TiO₂ composite and found that its photocatalytic
2 activity in degradation of methyl orange dye and 4-chlorine phenol was much higher
3 than that of pure TiO₂ [21]. Chu et al. reported that the photocatalytic properties of the
4 TiO₂ were enhanced from the UV to the visible after incorporation of
5 poly(3-hexylthiophene) (P3HT) [22]. Yi et al. have prepared polythiophene (PT)/TiO₂
6 composite and investigated its photocatalytic performance in the degradation of
7 methyl orange (MeO) [23]. These studies demonstrate that the introduction of a
8 conjugated polymer is an effective way to enhance the photocatalytic activity.

9 Among the conjugated polymers, poly(3-hexylthiophene) (P3HT) has attracted
10 much attention due to its high charge carrier mobility, dissolubility and processability,
11 long-term stability and broad absorption in visible region [24]. Especially, due to its
12 extended π -conjugated system, it's considered to be an excellent hole transporter.
13 Taking account of the efficient hole transporting ability of P3HT, we intended to
14 design a composite photocatalyst by combining P3HT with an inorganic
15 semiconductor, Bi₂WO₆, whose main oxidative species are holes [25, 26]. It is
16 expected that P3HT as an excellent hole conductor can transport the photo-generated
17 holes to the surface of the semiconductor quickly to participate in the oxidation of
18 pollutants, which can lead to an enhanced photocatalytic activity.

19 In this study, a novel P3HT/Bi₂WO₆ composite with high charge separation and
20 migration efficiency was designed. The P3HT/Bi₂WO₆ composite has a much higher
21 hole mobility than bare Bi₂WO₆, suggesting the high charge transfer ability of the
22 P3HT/Bi₂WO₆ composite. The photocatalytic activity evaluation, via the

1 photo-degradation of a model pollutant, rhodamine B (RhB) under simulated solar
2 light irradiation, demonstrated that the P3HT/Bi₂WO₆ composite showed much higher
3 photocatalytic activity than bare Bi₂WO₆. Moreover, the mechanism of the enhanced
4 photocatalytic activity was discussed in detail.

5 **2 Experimental**

6 **2.1 Sample preparation**

7 The reactants used in the experiment were analytical grade, without further
8 purification. Bi₂WO₆ photocatalyst was synthesized via a hydrothermal method. In a
9 typical process, 2 mmol of Bi(NO₃)₃·5H₂O was dissolved in 2 M nitric acid solution
10 to obtain a transparent solution A. Meanwhile, 1 mmol of Na₂WO₄·2H₂O was
11 dissolved in 30 mL of deionized water to get a transparent solution B. After that,
12 solution A and solution B were mixed together to obtain a white suspension. NaOH
13 solution was then added into the suspension until the pH value of the last suspension
14 was about 1-2. After being stirred for several hours, the suspension was added to a 50
15 mL Teflon-lined autoclave up to 80% of the total volume. The autoclave was sealed in
16 a stainless steel tank and heated at 160 °C for 20 h. Next, the autoclave was cooled to
17 room temperature naturally. The final products were washed with deionized water for
18 several times, and finally dried at 60 °C in air for 12 h.

19 P3HT/Bi₂WO₆ composites were prepared as follows: 0.3 g of the Bi₂WO₆ powder
20 was added into 10 mL of CH₃Cl and dispersed under ultrasonic vibration for 30 min.
21 Meanwhile, desired amount of P3HT was dissolved into 20 mL of CH₃Cl under
22 magnetic stirring. Subsequently, the two solutions were mixed and stirred for 24 h at
23 room temperature. Then the solvent was evaporated slowly in the vacuum and the

1 obtained powders were dried in an oven at 60 °C for 12 h. The loading amount of
2 P3HT was 0.25 wt%, 0.5 wt%, 0.75 wt% and 1 wt%, respectively.

3 **2.2 Characterization**

4 The phase and composition of the as-prepared samples were measured by X-ray
5 diffraction (XRD) studies using an X-ray diffractometer with Cu K α radiation under
6 40 kV and 20 mA and with the 2 θ ranging from 20° to 70° (Rigaku, Japan). The
7 morphologies and microstructures of the as-prepared samples were investigated by
8 transmission electron microscopy (TEM, FEI Tecnai). FT-IR spectra of the samples
9 were measured on a Nicolet iN10 (Thermo Fisher Scientific) FT-IR spectrometer. The
10 KBr pellets were prepared with dried samples and the spectrum was collected in the
11 range from 4000 to 400 cm⁻¹. UV-vis diffuse reflectance spectra (DRS) of the samples
12 were recorded with a UV-vis spectrophotometer (Cary Series UV-Vis-NIR
13 Spectrophotometer 5000) using BaSO₄ as a reference. The Hall mobility of the
14 samples were measured on a Lake Shore 775 HMS Matrix by pressing the powders
15 into a pellet. Photoelectrochemical measurements were performed in a three electrode
16 quartz cells with 0.1 M Na₂SO₄ electrolyte solution. Saturated calomel electrode (SCE)
17 and platinum wire were used as reference and counter electrodes, respectively.
18 Bi₂WO₆ and P3HT/Bi₂WO₆ film electrodes on ITO served as the working electrode.
19 The photoelectrochemical experiment results were recorded with an electrochemical
20 system (CHI-650E, China) using a 500 W Xe lamp as the light source.

21 **2.3 Photocatalytic test**

22 Photocatalytic activities of the P3HT/Bi₂WO₆ composites and Bi₂WO₆ were

1 evaluated by photocatalytic degradation of rhodamine B (RhB) under simulated solar
2 light irradiation. A 500 W Xe lamp with the wavelength of $\lambda > 290$ nm was used as
3 the light source. The experiments were conducted at room temperature as follows: 0.1
4 g of photocatalyst was added to 100 mL of RhB (10^{-5} mol L⁻¹) solution. Prior to
5 irradiation, the suspensions were magnetically stirred for an hour in the dark to ensure
6 the adsorption–desorption equilibrium between RhB and photocatalyst powders. At
7 fixed time intervals, 3 mL suspension was sampled and centrifuged to remove the
8 catalyst powders. After that, the supernatant was taken out to measure the absorption
9 spectral change of RhB through a UV–vis spectrophotometer (Cary Series
10 UV-Vis-NIR Spectrophotometer 5000) to monitor the photo-degradation rate. The
11 concentration change of RhB was determined by monitoring the optical intensity of
12 absorption spectra at 552 nm.

13 **3 Results and discussion**

14 **3.1. Crystal Structure**

15 The phase structures of the prepared products were investigated by a powder
16 X-ray diffractometer. The diffraction pattern in Fig. 1 shows that all the peaks can be
17 indexed to the orthorhombic phase of Bi₂WO₆ according to the JCPDS card no.
18 39-0256 and no other crystalline phase can be detected. Compared with the XRD
19 pattern of bare Bi₂WO₆, no distinct difference was observed on the P3HT/Bi₂WO₆
20 composites due to the low quality ratio of P3HT. This result implies that the
21 crystalline phase of Bi₂WO₆ has not been changed by the modification of P3HT.

22 **3.2. Morphology**

1 The morphologies and microstructures of P3HT, Bi₂WO₆ and the P3HT/Bi₂WO₆
2 composite (0.5 wt%) were revealed by TEM, as shown in Fig. 2. As shown in Fig.
3 2(a), P3HT exhibits a porous spongy morphology. Both Bi₂WO₆ and the
4 P3HT/Bi₂WO₆ composite display a two-dimensional plate-like morphology with
5 lateral sizes of 100–200 nm, as shown in the panoramic view in Fig. 2 (b) and Fig. 2
6 (c). However, closer observation of the P3HT/Bi₂WO₆ composite in Fig. 2 (d) and Fig.
7 2 (e) shows that some tiny nanocrystals with sizes of 5–10 nm are decorated on the
8 nanoplates, which could be ascribed to the existence of P3HT. Moreover, the
9 high-resolution transmission electron microscopy (HRTEM) in Fig. 2(f) shows clear
10 lattice spacing of the nanosheet matrix, which is consistent with the d-spacing (0.315
11 nm) of the (131) reflection of Bi₂WO₆.

12 3.3. FT-IR spectra analysis

13 Molecular structures of the resulting samples were characterized by FT-IR spectra
14 in the range from 4000 to 400 cm⁻¹, as shown in Fig. 3. The characteristic peaks of
15 P3HT and Bi₂WO₆ can be found in the spectra of the P3HT/Bi₂WO₆ composite. The
16 main characteristic peaks of P3HT appear in the spectrum of P3HT/Bi₂WO₆
17 composite as follows: The peak at 2926 cm⁻¹ is ascribed to the C–H stretching mode
18 of the thiophene rings. The peak at 2854 cm⁻¹ is attributed to the hexyl C–H
19 stretching absorption, while the absorption peak at 1459 is assigned to the C=C
20 stretching vibration on the thiophene ring [27]. Besides the characteristic peaks of
21 P3HT, main absorption bands at 400–1000 cm⁻¹, which are attributed to Bi–O, W–O
22 stretching, and W–O–W bridging stretching modes are also observed [28], which

1 indicates that the composite is composed of P3HT and Bi₂WO₆.

2 **3.4. UV–vis spectra**

3 The UV-vis diffuse reflectance spectra (DRS) of the P3HT/Bi₂WO₆ composites are
4 compared with that of bare Bi₂WO₆, as shown in Fig. 4. According to the spectra, bare
5 Bi₂WO₆ sample shows the characteristic spectrum with its fundamental absorption
6 edge at ca. 450 nm, corresponding to the band gap of 2.75 eV. It could be observed
7 that with the introduction of P3HT, the absorption intensity of the P3HT/Bi₂WO₆
8 composites increases remarkably, which is attributed to the electron transition from
9 the valence bond to the antibonding polaron state (π - π^* type) of P3HT [29].
10 Therefore, the P3HT/Bi₂WO₆ composite can harvest visible light effectively to
11 generate more photo-induced electrons and holes, which could result in higher visible
12 light photocatalytic activities.

14 **3.5. Photocatalytic activity**

15 In order to investigate the photocatalytic activity of the P3HT/Bi₂WO₆
16 composites, photo-degradation of RhB was carried out under simulated solar light
17 irradiation. The photo-degradation efficiencies of RhB as a function of irradiation
18 time in the presence of P3HT/Bi₂WO₆ composites compared to bare Bi₂WO₆ is shown
19 in Fig. 5. Blank test (RhB solution without any photocatalyst) shows that RhB
20 exhibits little photolysis, which demonstrates that RhB is quite stable under simulated
21 solar light. Obviously, the introduction of P3HT into Bi₂WO₆ could significantly
22 enhance the photocatalytic activity of the composite. When the loading amount of
23 P3HT is 0.5 wt%, the sample shows the best photocatalytic performance, which could

1 degrade RhB completely within 5 min. When the loading amount of P3HT further
2 increases to 0.75 wt% and 0.1 wt%, the photocatalytic activities of the composites
3 decrease as compared to that of 0.5 wt%, but still higher than that of bare Bi₂WO₆,
4 which suggests that there is an optimum loading content for P3HT. It is estimated that
5 when the loading amount of P3HT increases, more active reaction sites on the surface
6 of Bi₂WO₆ are covered, and the photocatalytic activities decrease. Therefore,
7 appropriate amount of P3HT could enhance the photocatalytic activity of Bi₂WO₆
8 effectively.

9 The stability of the photocatalyst is a main factor determining the potential for its
10 practical application. In order to check the stability of the P3HT/Bi₂WO₆ composite,
11 the photocatalyst was recycled and characterized by TEM and FT-IR spectra. As
12 shown in Fig. 6(a), the morphology of the recycled P3HT/Bi₂WO₆ composite does not
13 show obvious change, with the P3HT nanoparticles decorated on the Bi₂WO₆
14 nanoplates. Moreover, the FT-IR spectrum of the recycled P3HT/Bi₂WO₆ composite
15 shown in Fig. 6(b) indicates that the characteristic peaks corresponding to the C–H
16 stretching mode of the thiophene rings, the hexyl C–H stretching absorption, and the
17 C=C stretching vibration of P3HT molecule could be observed. These results
18 demonstrate that the P3HT/Bi₂WO₆ composite is stable and is not photodegraded with
19 time.

20 **3.6. Mechanism of enhancement of photocatalytic activity**

21 The photocatalytic process involves the generation of charge carriers such as
22 electrons and holes induced by light, which then transfer to the surface of the

1 semiconductor to participate in the oxidation of pollutants. Therefore, an ideal
2 photocatalyst should have both a high charge separation efficiency and a high charge
3 migration rate. The hybridization of P3HT could contribute to these two parameters in
4 such two ways: first, P3HT is a p type semiconductor with a bandgap of 1.9-2.1 eV
5 [30], while Bi_2WO_6 is an n type semiconductor with a bandgap of ca. 2.8 eV [31].
6 Therefore, when Bi_2WO_6 is hybridized by P3HT, a p-n heterojunction would be
7 formed and the charge carriers would diffuse in the opposite direction to form an
8 internal electric field in the direction from n-type Bi_2WO_6 to p-type P3HT at the
9 heterojunction interface. Under simulated solar light irradiation, the P3HT polymer
10 absorbs photons and promotes an electron from the ground state into an excited state.
11 The polymer π -orbital becomes the highest occupied molecular orbital (HOMO) and
12 the π^* -orbital becomes the lowest unoccupied molecular orbital (LUMO).
13 Simultaneously, electrons can be excited to the conduction band (CB) and leave holes
14 in the valence band (VB) of Bi_2WO_6 . Since the LUMO level of P3HT is more
15 negative than the conduction band edge of Bi_2WO_6 [30, 32], the photo-induced
16 electrons of P3HT could transfer easily to Bi_2WO_6 via the well developed interface,
17 while the photo-generated holes are effectively collected in the π -orbital of P3HT, as
18 shown in Fig. 7. Due to the formation of the internal electric field, the migration of
19 photo-generated carriers is promoted. In this way, the photo-induced charge carriers
20 are separated effectively, resulting in higher photocatalytic activity.

21 Photocurrent is an effective method to reflect the generation, separation and
22 migration efficiency of photogenerated charge carriers. Fig. 8 shows the photocurrent

1 of Bi₂WO₆ and P3HT/Bi₂WO₆ samples under simulated solar light. It can be seen that
2 the photocurrent generated from P3HT/Bi₂WO₆ composite is larger than that of pure
3 Bi₂WO₆. The increased photocurrent could be attributed to the higher separation
4 efficiency of photogenerated electron-hole pairs, which is beneficial to the
5 enhancement of photocatalytic activity.

6 More importantly, due to its special conjugated structure, P3HT is an excellent
7 hole conductor, and the photo-generated holes can be transported easily through the
8 π -conjugated bond of P3HT. Coincidentally, the main oxidative species in the Bi₂WO₆
9 photocatalysis system are holes. To further confirm this, the trapping experiments of
10 radicals were performed using tert-butyl alcohol (tBuOH) as a hydroxyl radical
11 scavenger, and EDTA-2Na as a hole radical scavenger, respectively [33, 34]. As
12 shown in Fig. 9, the photocatalytic activity of P3HT/Bi₂WO₆ is hardly inhibited by
13 adding free radical scavenger, while the photocatalytic activity of P3HT/Bi₂WO₆ is
14 severely suppressed by the addition of hole scavenger. This indicates that the
15 photo-generated holes are the major oxidative species in the P3HT/Bi₂WO₆ system on
16 the degradation of RhB. The high hole carrier mobility of P3HT can enable the
17 photo-generated holes to migrate to composite/solution interface easily to participate
18 in the oxidation reaction, which is beneficial to the enhancement of the photocatalytic
19 activity. In order to compare the charge transfer ability of Bi₂WO₆ and P3HT/Bi₂WO₆,
20 the hall mobility of the two samples were tested. The result shows that the hall
21 mobility of test samples of Bi₂WO₆ and P3HT/Bi₂WO₆ (0.5wt%) are 3.0159×10^2
22 cm^2/Vs and $4.7197 \times 10^2 \text{ cm}^2/\text{Vs}$, respectively, which indicates that hybridizing P3HT

1 can improve the charge transfer rate of Bi_2WO_6 effectively. Therefore, due to the high
2 charge separation and transportation efficiency, the P3HT/ Bi_2WO_6 composite exhibits
3 excellent photocatalytic performance.

4 **4 Conclusion**

5 In summary, a novel P3HT/ Bi_2WO_6 composite photocatalyst with high charge
6 separation and transportation efficiency was synthesized. The composite photocatalyst
7 exhibited excellent photocatalytic activity in degradation of RhB under simulated
8 solar light irradiation, which was much higher than that of bare Bi_2WO_6 . The
9 enhanced activity can be attributed to the effective separation of electron–holes pairs
10 due to the formation of the internal electric field between P3HT and Bi_2WO_6 , as well
11 as the high hole carrier mobility of P3HT, which can transport the photo-generated
12 holes to composite/solution interface quickly to participate in the oxidation of
13 pollutants. Such a composite photocatalyst is promising for water purification and
14 environmental remediation.

15 **Acknowledgements**

16 This work was supported by the National Natural Science Foundation of China
17 (51402194), the Shanghai Science and Technology Committee (14YF1410700), the
18 Shanghai Education Commission (15ZZ097), and the Program for Professor of
19 Special Appointment (Eastern Scholar) at Shanghai Institutions of Higher Learning
20 (4521ZK120053002).

21

1 **References**

- 2 [1] A. Hagfeldt and M. Gratzel, *Chem. Rev.*, 1995, 95, 49–68.
- 3 [2] A. Kubacka, M. Fernández-García and G. Colón, *Chem. Rev.*, 2012, 112,
4 1555–1614.
- 5 [3] J. S. Zhang, M. W. Zhang, R. Q. Sun and X. C. Wang, *Angew. Chem.*, 2012, 124,
6 10292–10296.
- 7 [4] M. R. Hoffmann, S. T. Martin, W. Choi and D. W. Bahnemann, *Chem. Rev.*, 1995,
8 95, 69–96.
- 9 [5] K. Maeda and K. Domen, *J. Phys. Chem. Lett.*, 2010, **1**, 2655–2661.
- 10 [6] M. Schwab, M. Hamburger, X. Feng, J. Shu, H. Spiess, X. Wang, M. Antonietti
11 and K. Mullen, *Chem. Commun.*, 2010, 46, 8932–8934.
- 12 [7] H. Yan, J. Yang, G. Ma, G. Wu, X. Zong, Z. Lei, J. Shi and C. Li, *J. Catal.*, 2009,
13 266, 165–168.
- 14 [8] K. Maeda, A. Xiong, T. Yoshinaga, T. Ikeda, N. Sakamoto, T. Hisatomi, M.
15 Takashima, D. Lu, M. Kanehara, T. Setoyama, T. Teranishi and K. Domen, *Angew.*
16 *Chem., Int. Ed.*, 2010, 49, 4190–4193.
- 17 [9] Y. F. Liu, W. Q. Yao, D. Liu, R. L. Zong, M. Zhang, X. G. Ma and Y. F. Zhu, *Appl.*
18 *Catal. B: Environ.*, 2015, 163, 547–553.
- 19 [10] Y. Liu, F. Xin, F. Wang, S. Luo and X. Yin, *J. Alloys. Compd.*, 2010, 498,
20 179–184.
- 21 [11] D. Yue, D. M. Chen, Z. H. Wang, H. Ding, R. L. Zong and Y. F. Zhu, *Phys. Chem.*
22 *Chem. Phys.*, 2014, 16, 26314–26321.

- 1 [12] W. H. He, R. R. Wang, L. Zhang, J. Zhu, X. Xiang and F. Li, *J. Mater. Chem. A*,
2 2015, 3, 17977–17982.
- 3 [13] X. Xiang, L. S. Xie, Z. W. Li and F. Li, *Chem. Eng. J.*, 2013, 221, 222–229.
- 4 [14] W. H. He, Y. Yang, L. R. Wang, J. J. Yang, X. Xiang, D. P. Yan and F. Li,
5 *ChemSusChem*, 2015, 8, 1568–1576.
- 6 [15] H. J. Yan and Y. Huang, *Chem. Commun.*, 2011, 47, 4168–4170.
- 7 [16] Y. W. Su, W. H. Lin, Y. J. Hsu and K. H. Wei, *Small*, 2014, 10, 4427–4442.
- 8 [17] K. R. Reddy, M. Hassan and V. G. Gomes, *Appl. Catal. A: Gen.*, 2015, 489, 1–16.
- 9 [18] I. Gonzalez-Valls and M. Lira-Cantu, *Energy Environ. Sci.*, 2009, 2, 19–34.
- 10 [19] B. Kippelen and J. Bredas, *Energy Environ. Sci.*, 2009, 2, 251–261.
- 11 [20] M. Helgesen, R. Søndergaard and F.C. Krebs, *J. Mater. Chem.*, 2010, 20, 36–60.
- 12 [21] Y. M. Lin, D. Z. Li, J. H. Hu, G. C. Xiao, J. X. Wang, W. J. Li and X. Z. Fu, *J.*
13 *Phys. Chem. C*, 2012, 116, 5764–5772.
- 14 [22] J. H. Huang, M. A. Ibrahim and C. W. Chu, *RSC Adv.*, 2013, 3, 26438–26442.
- 15 [23] Y. Zhu, S. Xu and D. Yi, *React. Funct. Polym.*, 2010, 70, 282–287.
- 16 [24] D. E. Motaung, G. F. Malgas, C. J. Arendse, S. E. Mavundla, C. J. Oliphant and
17 D. Knoesen, *Sol. Energy Mater. Sol. Cells*, 2009, 93, 1674–1680.
- 18 [25] H. B. Fu, C. S. Pan, W. Q. Yao and Y. F. Zhu, *J. Phys. Chem. B*, 2005, 109,
19 22432–22439.
- 20 [26] Y. J. Wang, X. J. Bai, C. S. Pan, J. He and Y. F. Zhu, *J. Mater. Chem.*, 2012, 22,
21 11568–11573.
- 22 [27] D. S. Wang, J. Zhang, Q. Z. Luo, X. Y. Li, Y. D. Duan and J. An, *J. Hazard.*

- 1 *Mater.*, 2009, 169, 546–550.
- 2 [28] Z. J. Zhang, W. Z. Wang and E. P. Gao, *J. Mater. Sci.*, 2014, 49, 7325–7332.
- 3 [29] Y. F. Zhu and Y. Dan, *Sol. Energy Mater. Sol. Cells*, 2010, 94, 1658–1664.
- 4 [30] X. J. Bai, C. P. Sun, S. L. Wu and Y. F. Zhu, *J. Mater. Chem. A*, 2015, 3,
5 2741–2747.
- 6 [31] Q. Xiao, J. Zhang, C. Xiao and X. K. Tan, *Catal. Commun.*, 2008, 9, 1247–1253.
- 7 [32] Z. J. Zhang, W. Z. Wang, L. Wang and S. M. Sun, *ACS Appl. Mater. Interfaces*,
8 2012, 4, 593–597.
- 9 [33] M. Zhang, W. Q. Yao, Y. H. Lv, X. J. Bai, Y. F. Liu, W. J. Jiang and Y. F. Zhu, *J.*
10 *Mater. Chem. A*, 2014, 2, 11432–11438.
- 11 [34] Y. Y. Zhu, Y. F. Liu, Y. H. Lv, Q. Ling, D. Liu and Y. F. Zhu, *J. Mater. Chem. A*,
12 2014, 2, 13041–13048.
- 13

1 **Figure Captions**

2 **Fig. 1** XRD patterns of the as-prepared products.

3 **Fig. 2 (a)** TEM image of P3HT; (b) TEM image of Bi_2WO_6 ; (c) and (d) TEM images
4 of the P3HT/ Bi_2WO_6 composite (0.5 wt%); (e) and (f) high resolution TEM images of
5 the P3HT/ Bi_2WO_6 composite (0.5 wt%).

6 **Fig. 3** FT-IR spectra of P3HT, Bi_2WO_6 and P3HT/ Bi_2WO_6 composite (0.5 wt%).

7 **Fig. 4** UV–vis diffuse reflectance spectra of the as-prepared samples.

8 **Fig. 5** Degradation efficiency of RhB as a function of time by the as-prepared samples
9 under simulated solar light irradiation.

10 **Fig. 6** TEM image (a) and FT-IR spectrum (b) of the recycled P3HT/ Bi_2WO_6
11 composite.

12 **Fig. 7** Schematic representation of interfacial charge separation in P3HT/ Bi_2WO_6
13 composite.

14 **Fig. 8** Photocurrent response for Bi_2WO_6 and P3HT/ Bi_2WO_6 composite.

15 **Fig. 9** Photocatalytic degradation of RhB by P3HT/ Bi_2WO_6 composite photocatalyst
16 with different scavengers under simulated solar light irradiation.

17

18

19

20

1
2
3
4
5
6
7
8
9
10
11
12
13
14
15
16
17
18
19
20

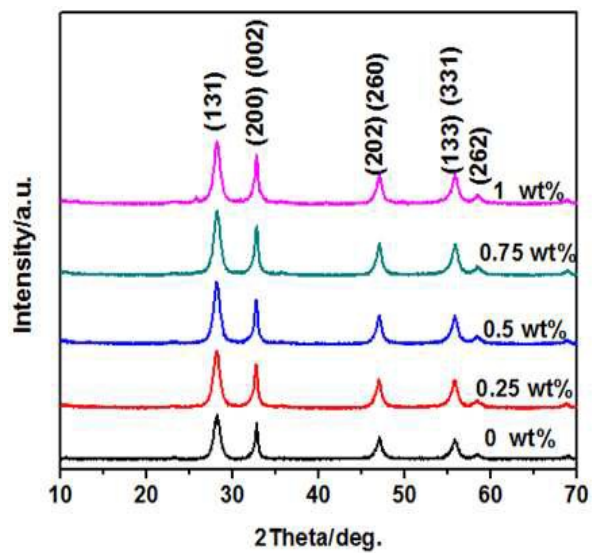


Fig. 1

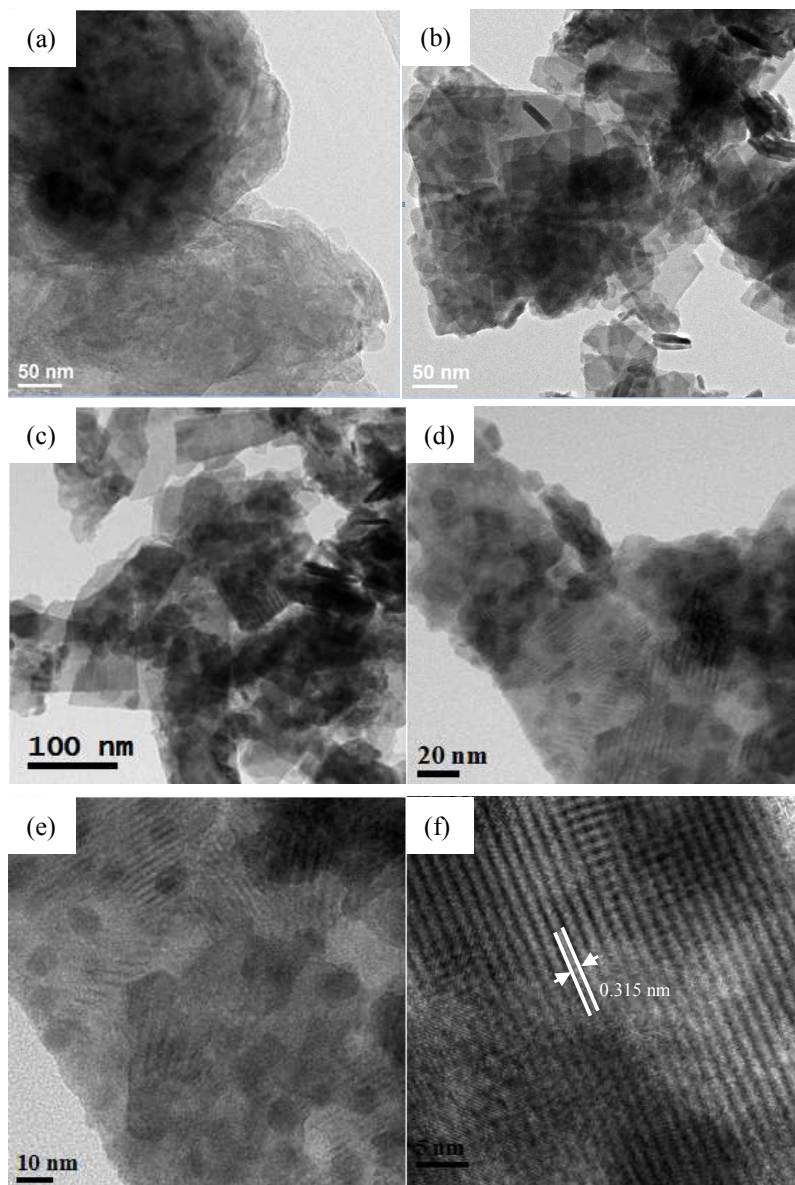


Fig. 2

1
2
3
4
5
6
7
8
9
10
11
12
13
14
15
16
17
18
19
20

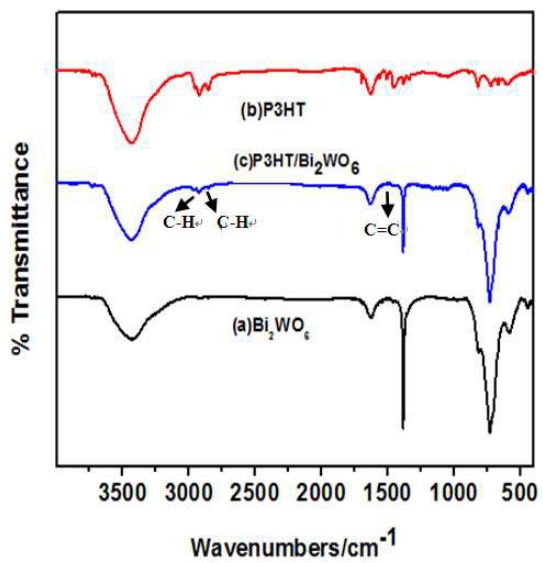


Fig. 3

1
2
3
4
5
6
7
8
9
10
11
12
13
14
15
16
17
18
19

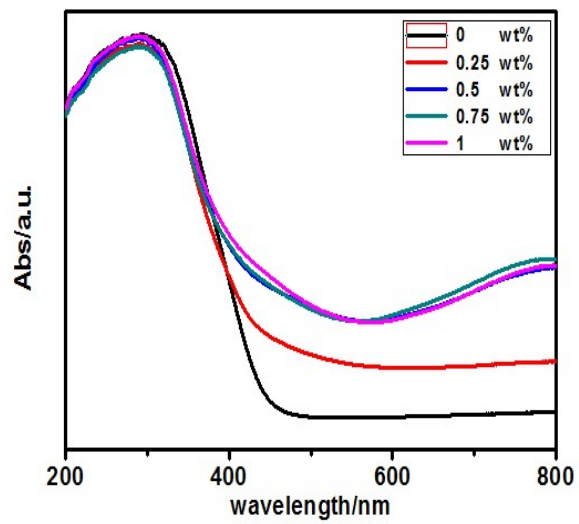


Fig. 4

1
2
3
4
5
6
7
8
9
10
11
12
13
14
15
16
17
18
19

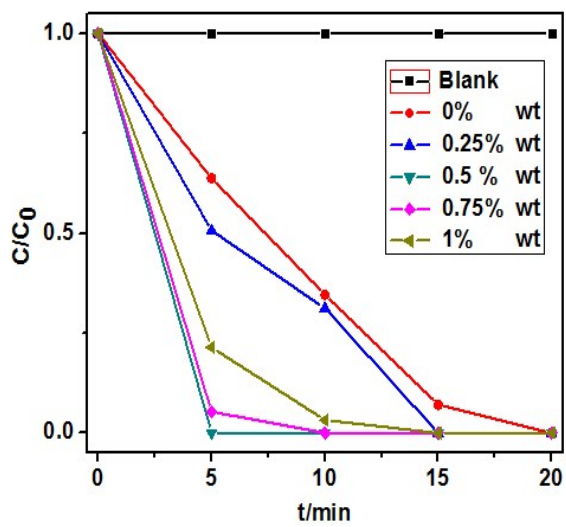


Fig. 5

1
2
3
4
5
6
7
8
9
10
11
12
13
14
15
16

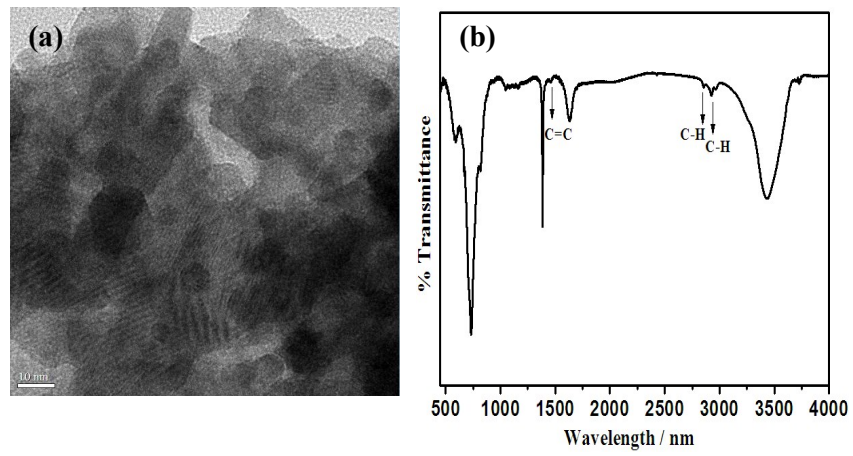


Fig. 6

1
2
3
4
5
6
7
8
9
10
11
12
13
14
15
16
17
18

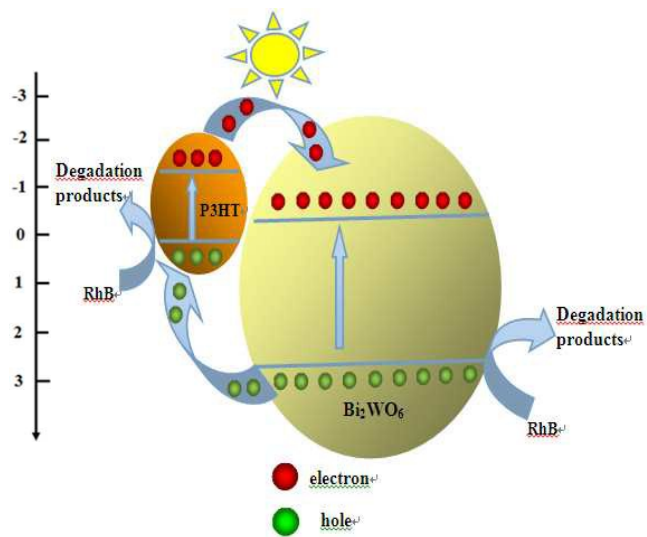


Fig. 7

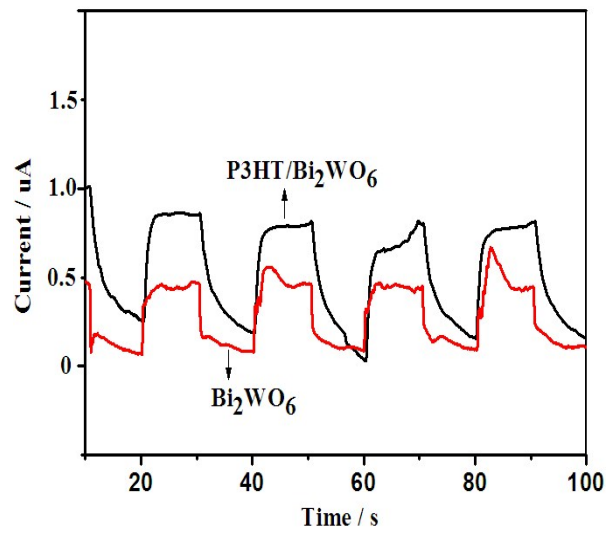


Fig. 8

1
2
3
4
5
6
7
8
9
10
11
12
13
14
15
16
17
18
19
20
21

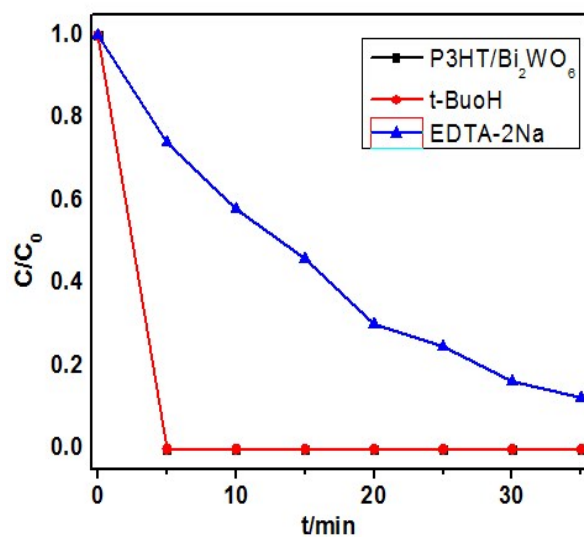
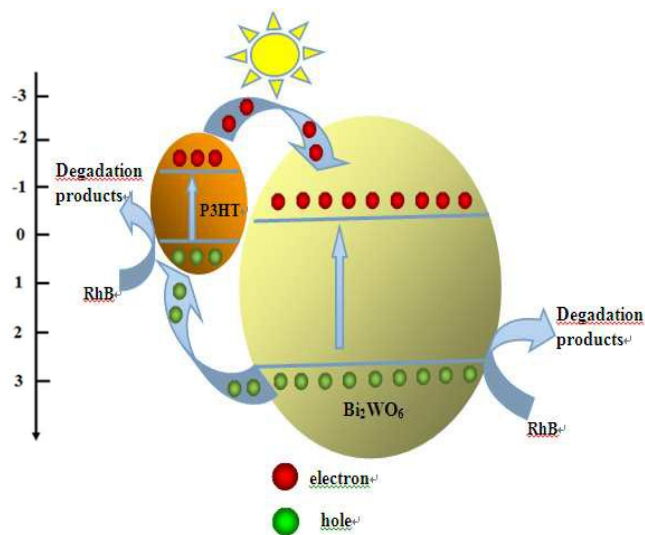


Fig. 9



A novel P3HT/Bi₂WO₆ composite photocatalyst with high charge separation and migration efficiency was designed, which exhibited excellent photocatalytic performance in degradation of RhB under simulated solar light irradiation.